

**Controlling the flow of light using inhomogeneous effective gauge  
field that emerges from dynamic modulation: Supplementary**

**Information**

Kejie Fang

*Department of Physics, Stanford University, Stanford, California 94305, USA*

Shanhui Fan

*Department of Electrical Engineering,  
Stanford University, Stanford, California 94305, USA*

## I. EXPERIMENTAL IMPLEMENTATION

We discuss the physical implementation of the Hamiltonian of Eq. (1). This Hamiltonian describes a resonator lattice as schematically shown in Fig. S1(a), where the coupling constants between nearest-neighbor resonators are modulated dynamically in the form of  $V \cos(\Omega t + \phi)$ . Conceptually, to implement this Hamiltonian, the key is to achieve such dynamical coupling between two resonators that form a single bond (dashed box in Fig. S1(a)).

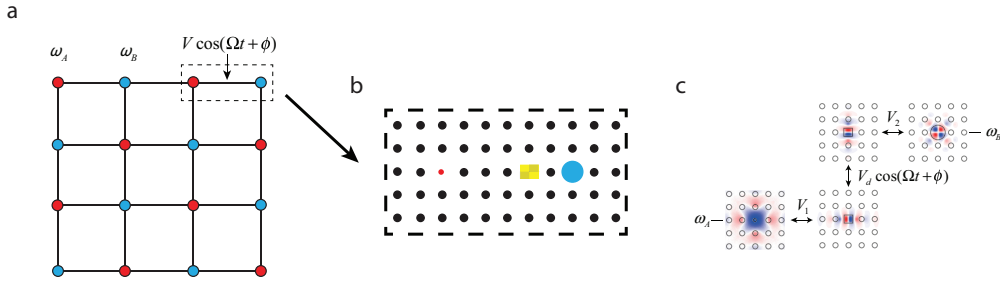


FIG. S1. **a** A photonic resonator lattice with harmonically modulated nearest-neighbor coupling. The red and blue dots correspond to resonators  $A$  and  $B$ , respectively. **b** A photonic crystal platform for implementing the dynamical coupling on a single bond between two resonators (dashed box in **a**). All dots here represent dielectric rods. The black dots here represent rods that create a photonic crystal. The periodicity here is approximately 540 nm for light with free space wavelength of  $1.55 \mu\text{m}$ . The red and blue dots are rods with modified radii, and correspond to resonators  $A$  and  $B$ , respectively. Resonator  $A$  supports a monopole mode. Resonator  $B$  supports a quadrupole mode. The yellow region is a coupling resonator supporting a pair of dipole modes. Its dielectric constant is modulated as a function of time. The details of the parameters can be found in Ref. [S1]. **c** Level diagram illustrating the field distributions, frequencies, and coupling, for the resonances in **b**.

Here we introduce a physical structure based on point-defect resonators in a photonic crystal, as shown in Fig. S1(b), that provides such dynamic coupling. The structure in Fig. S1(b) contains resonators  $A$  and  $B$ , supporting a monopole mode at frequency  $\omega_A$ , and a quadrupole mode at frequency  $\omega_B$ , respectively, as shown in Fig. S1(c). Due to the frequency and symmetry mismatch between these two modes, they do not couple statically. To introduce a dynamic coupling between them, we place an additional coupling resonator between resonators  $A$  and  $B$ . The coupling resonator supports a pair of dipole modes, at frequencies  $\omega_A$  and  $\omega_B$  respectively (Fig. S1(c)). The dielectric constant of the coupling resonator is modulated harmonically at a frequency  $\Omega = \omega_B - \omega_A$ , with a form

$$\Delta\epsilon(\vec{r}, t) = \delta(\vec{r})\cos(\Omega t + \phi). \quad (\text{S1})$$

The structure in Fig. S1(b) is therefore described by a four-mode coupled mode theory,

$$\frac{da_A}{dt} = i\omega_A a_A + iV_1 a_{p_x}, \quad (\text{S2})$$

$$\frac{da_{p_x}}{dt} = i\omega_A a_{p_x} + iV_1 a_A + iV_d \cos(\Omega t + \phi) a_{p_y}, \quad (\text{S3})$$

$$\frac{da_{p_y}}{dt} = i\omega_B a_{p_y} + iV_2 a_B + iV_d \cos(\Omega t + \phi) a_{p_x}, \quad (\text{S4})$$

$$\frac{da_B}{dt} = i\omega_B a_B + iV_2 a_{p_y}, \quad (\text{S5})$$

where  $a_A$  and  $a_B$  are the amplitudes in resonators  $A$  and  $B$  respectively,  $a_{p_x}$  and  $a_{p_y}$  are the amplitudes of the two modes in the coupling resonator. Under the condition  $V_d \ll V_1, V_2, \Omega$ , these equations can be further reduced to a two-mode coupled-mode theory equations,

$$\frac{d\tilde{a}_A}{dt} = i\omega_A \tilde{a}_A + i\frac{V_d}{2} \cos(\Omega t + \phi) \tilde{a}_B, \quad (\text{S6})$$

$$\frac{d\tilde{a}_B}{dt} = i\omega_B \tilde{a}_B + i\frac{V_d}{2} \cos(\Omega t + \phi) \tilde{a}_A, \quad (\text{S7})$$

where  $\tilde{a}_{A(B)} = e^{iV_1(2)t} a_{A(B)}$  (Supplementary Information in Ref. [S1]). The description of the effect of modulations on such a four-mode resonator system, in terms of the two-mode

coupled mode theory, has been validated by direct finite-difference time-domain simulations as discussed in details in Ref. [S1].

We therefore see that the dielectric constant modulation of the coupling resonator generates a dynamic coupling of the required form  $V \cos(\Omega t + \phi)$  between the two single-mode resonators. Here the dynamic coupling constant is related to the dielectric constant modulation strength via

$$V = \frac{V_d}{2} = \frac{\sqrt{\omega_A \omega_B}}{8} \frac{\int d\vec{r} \delta(\vec{r}) \vec{E}_1^* \cdot \vec{E}_2}{\sqrt{\int d\vec{r} \epsilon(\vec{r}) |\vec{E}_1|^2} \sqrt{\int d\vec{r} \epsilon(\vec{r}) |\vec{E}_2|^2}}, \quad (\text{S8})$$

where  $\vec{E}_{1,2}$  are the normal electric fields of the two dipole modes. And the phase  $\phi$  is the same as the phase of the dielectric constant modulation. One should not confuse the phase  $\phi$  of the dielectric constant modulation, which physically corresponds to the phase of the RF wave that generates the modulation, with the phase that the optical wave acquire as it propagates through the medium. We note that the gauge field arises from the spatial distribution of the modulation phase  $\phi$ , which can be arbitrarily set.

In general, the achievable dielectric constant modulation is weak, leading to a limited magnitude of  $V$ , which in turn places a constraint of the quality factor  $Q$  of the resonators. In order that the photon amplitude does not diminish significantly after the beam steering, we require  $V > \omega_{A,B}/Q$ . This requirement is sufficient for the beam focusing effect shown in Fig. 4. For a modest modulation  $\Delta\epsilon/\epsilon \approx 5 \times 10^{-5}$ , we find  $Q \approx 10^5$ , which is achievable using the state-of-the-art photonic crystal resonator arrays [S2].

## II. EFFECT OF DISORDER IN RESONANT FREQUENCIES

We consider the effect of disorders that might be induced due to the modulation of the resonant cavities. The frequency of resonators can shift in the presence of dynamic

modulation, given by a similar formula as Eq. (S8):

$$\delta\omega = \frac{\omega}{8} \frac{\int d\vec{r} \delta(\vec{r}) \vec{E}^* \cdot \vec{E}}{\int d\vec{r} \epsilon(\vec{r}) |\vec{E}|^2}, \quad (\text{S9})$$

where  $\vec{E}$  is the electric field of the resonance mode. The frequency shift can be in principle eliminated by adopting an odd-symmetric profile  $\delta(\vec{r})$  of the modulation, as of the case of Fig. S1b, since thus the numerator of Eq. (S9) will be zero. In the general case, where the symmetry of the modulation is not perfect, the modulation will introduce additional frequency fluctuation in the resonators. Here, we consider the general case where such kind of frequency shift is present, and show the beam propagation effects demonstrated in the paper are robust to reasonable amount of resonant frequency fluctuation as induced by dynamic modulation.

To simulate the effect of such a fluctuation in resonator frequency, we add a frequency shift term to each resonator in the lattice of Fig. S1a,  $\delta\omega \cos(\Omega t + \phi_r)$ , where  $\delta\omega$  is given by Eq. (S9),  $\Omega$  is the modulation frequency, and  $\phi_r$  is a phase taking a random value between 0 and  $2\pi$ , and is generated for each resonator individually. Thus, the dynamically modulated lattice is dressed with time-dependent frequency disorders. The Hamiltonian (Eq. (1)) of the lattice is modified to be

$$H(t) = \sum_i (\omega_A + \delta\omega \cos(\Omega t + \phi_{ri})) a_i^\dagger a_i + \sum_j (\omega_B + \delta\omega \cos(\Omega t + \phi_{rj})) b_j^\dagger b_j \quad (\text{S10})$$

$$+ \sum_{\langle ij \rangle} V \cos(\Omega t + \phi_{ij}) (a_i^\dagger b_j + b_j^\dagger a_i).$$

The Hamiltonian describes a resonator system where the instantaneous resonance frequencies fluctuate in both space and time.

Using Eq. (2) and the Hamiltonian of Eq. (S10), Fig. S2 a and b show the beam trajectories corresponding to the refraction (Fig. 2c) and focusing (Fig. 4a) effects in the presence of the frequency disorders respectively, with  $\delta\omega = V$ . The major features of

the trajectory are clearly preserved for such a disorder. Such robustness arises from the fact that the non-reciprocal phase induced by the modulation phase persists as long as the rotating wave approximation holds. A similar result also shows the effects are robust to static frequency disorders due to device fabrication.

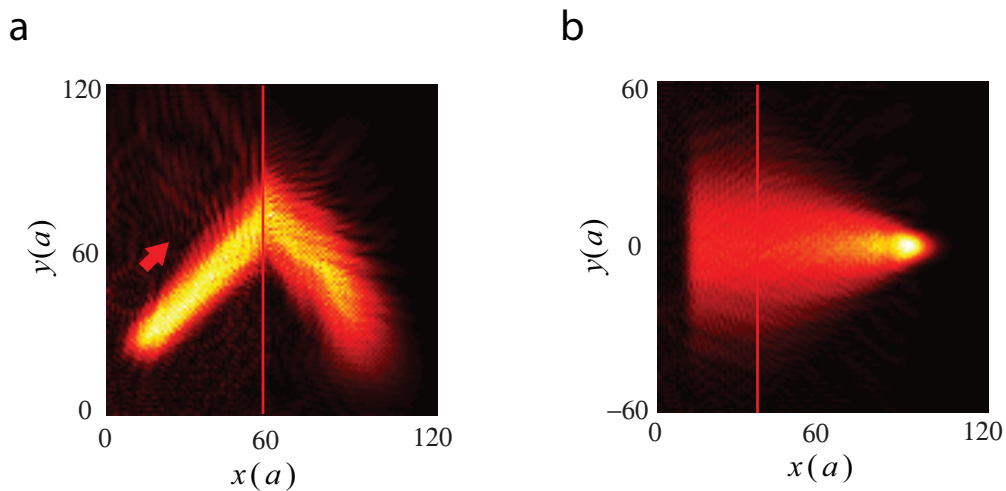


FIG. S2. Beam trajectories in the presence of disorders of resonant frequency: **a** refraction **b** focusing.

---

[S1] K. Fang, Z. Yu, and S. Fan, *Nature Photonics* **6**, 782 (2012).

[S2] M. Notomi, E. Kuramochi, and T. Tanabe, *Nature Photonics*. **2**, 741 (2008).